Asymptotic boundary element methods for thin conducting sheets in two dimensions

K. Schmidt[1] and Ralf Hiptmair[2]

[1]DFG Research Center Matheon, Technische Universität Berlin, 10623 Berlin, Germany
[2]Seminar for Applied Mathematics, ETH Zurich, 8092 Zürich, Switzerland

Shielding sheets are commonly used in the protection of electronic devices. With their large aspect ratios they become a serious issue for the direct application of boundary element methods due to the occurring almost singular integrals. Impedance transmission conditions allow for boundary element formulations where only sheet mid-line has to be triangulated. We propose and analyse boundary element methods of second kind for impedance transmission conditions of two different types for the time-harmonic eddy current problem in two dimensions. In numerical experiments we study the effect on the magnetic shielding efficiency of the discretisation error due the boundary element discretisation and the modelling error due to the impedance transmission condition.

Index Terms—**Computational electromagnetics, Eddy currents, Electromagnetic shielding, Integral equations.**

I. Introduction

The time-harmonic eddy current model [1] (time convention $\exp(-i\omega t)$, $\omega > 0$) in the transverse magnetic (TM) mode in two dimensions reads

$$\mathbf{curl}_{2D}\, e(\mathbf{x}) = \mathrm{i}\omega\mu(\mathbf{x})\mathbf{h}(\mathbf{x}), \tag{1}$$

$$\mathrm{curl}_{2D}\, \mathbf{h}(\mathbf{x}) = \sigma(\mathbf{x})e(\mathbf{x}) + j_0(\mathbf{x}), \tag{2}$$

where the 2D rotation operators are defined by $\mathbf{curl}_{2D} = (\partial_y, -\partial_x)^\top$ and $\mathrm{curl}_{2D} = (-\partial_y, \partial_x)$, e and $\mathbf{h}$ denote the out-of-plane electric and in-plane magnetic fields, σ is the (constant) conductivity of the thin sheet Ω_{int} of thickness d, and we assume it to vanish elsewhere for simplicity, μ is the permeability (taking the constant value μ_{int} inside the sheet and μ_{ext} outside), and j_0 is the out-of-plane imposed current whose location is well separated from the conductor. Inserting (1) in (2) outside the thin conductor and using the identity $\mathrm{curl}_{2D}\,\mathbf{curl}_{2D} = -\Delta$ we obtain

$$-\Delta\, e = \mathrm{i}\omega\mu_{\mathrm{ext}} j_0, \tag{3}$$

where we assume non-magnetic material outside the sheet, *e. g.*, air. We consider (3) in the infinite domain $\mathbb{R}^2\backslash\Omega_{\mathrm{int}}$ with suitable decay conditions. The thin sheet is assumed to be composed of all points with distance less than $d/2$ from its mid-line Γ, which shall be continuously differentiable. We call $\mathbf{n}$ the normalised normal vector on Γ, see Fig. 1, and $\boldsymbol{\tau} = (n_2, -n_1)^\top$ the normalised tangential vector.

The electric field has an exponentially behaviour in thickness direction inside the thin sheet, which is known as skin effect and can be quantified by the skin depth $\delta = \sqrt{2/(\omega\mu_{\mathrm{int}}\sigma)}$. For convenience we call $\gamma = (-1 + \mathrm{i})/\delta = \sqrt{-i\omega\mu_{\mathrm{int}}\sigma}$. We denote the case where the sheet thickness is much smaller than the skin depth as "low frequency case" and the case where the skin depth is much smaller than the sheet thickness as "high frequency case".

The induced currents σe in the thin sheets diminish the fields behind the thin conductor. In observation points $\mathbf{x}_j$ in $\mathbb{R}^2\backslash\Omega_{\mathrm{int}}$ we can compute the magnetic shielding efficiency [2] (measured in decibels (dB))

$$\mathrm{SE}(\mathbf{x}_j) = 20\log_{10}\frac{|\mathbf{h}_0(\mathbf{x}_j)|}{|\mathbf{h}(\mathbf{x}_j)|}, \tag{4}$$

where $\mathbf{h}_0$ is the magnetic field in absence of a conducting sheet, *i. e.*, $\sigma \equiv 0$ in Ω_{int}.

II. Impedance transmission conditions

Several impedance transmission conditions (ITCs) have been derived for the time-harmonic eddy-current model. Models with transmission conditions provide approximations $\tilde{e}$, $\widetilde{\mathbf{h}}$ to the solution e, $\mathbf{h}$ of the original model with resolved thin sheet, which are defined even up to the mid-line of the sheet, hence, $\mathbb{R}^2\backslash\Gamma$. The tangential components of $\tilde{e}$, $\widetilde{\mathbf{h}}\cdot\boldsymbol{\tau}$ may take different values $\tilde{e}^\pm$ and $\widetilde{\mathbf{h}}^\pm\cdot\boldsymbol{\tau}$ on both sides of Γ, and we define the jumps and mean values

$$[\tilde{e}] = \tilde{e}^+ - \tilde{e}^-, \qquad \{\tilde{e}\} = \tfrac{1}{2}\left(\tilde{e}^+ + \tilde{e}^-\right), \tag{5a}$$

$$\left[\widetilde{\mathbf{h}}\cdot\boldsymbol{\tau}\right] = \left(\widetilde{\mathbf{h}}^+ - \widetilde{\mathbf{h}}^-\right)\cdot\boldsymbol{\tau}, \qquad \left\{\widetilde{\mathbf{h}}\cdot\boldsymbol{\tau}\right\} = \tfrac{1}{2}\left(\widetilde{\mathbf{h}}^+ + \widetilde{\mathbf{h}}^-\right)\cdot\boldsymbol{\tau}. \tag{5b}$$

Probably the first ITCs were proposed by Levi-Civita [3] in 1902, which read for the TM mode

$$[\tilde{e}] = 0, \qquad [\widetilde{\mathbf{h}}\cdot\boldsymbol{\tau}] = -d\sigma\{\tilde{e}\}. \tag{6}$$

These conditions are so simple, that they seem to be mostly used as "physically meaningful", at least for the low frequency case, mostly without giving a reference. Note, that $d\sigma$ can be replaced by $\int_{-d/2}^{+d/2}\sigma(s)\,\mathrm{d}s$ if the conductivity σ varies in thickness direction s. In [4] it has been shown that (6) is the limit $d \to 0$ if the quantity $\omega\sigma$ is scaled like $1/d$, which corresponds to asymptotically constant shielding. The conditions (6) are the member of order zero of a family of impedance transmission conditions ITC-1-N derived by asymptotic expansions [5], and, hence, we call them ITC-1-0. In [6] it has been shown that the ITC-1-0 are robust with respect to the frequency and can be used for both the low and high frequency case.

Other impedance transmission conditions are the shielding element [7], the thin sheet conditions [8], [9], [10] and a second family ITC-2-N derived by asymptotic expansions [6]. We refer to [6] for an overview on ITCs for the eddy-current model.

Note, that the above mentioned ITCs are derived for smooth sheets without kinks or endings, *e. g.*, by neglecting derivatives along the sheet. In this paper we consider two types of ITCs.

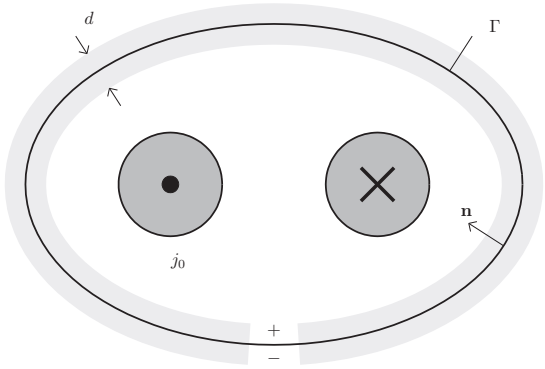

Figure 1: Limit geometry for $d \to 0$ for the impedance conditions and integral equations. The original sheet of thickness d is indicated with light shading.

A. Impedance transmission conditions of type I

For the simplest impedance transmission conditions the electric field is continuous over Γ and the jump of the magnetic field is proportional to the electric field. Using (1) we can write directly for the (mean of the) electric field

$$[\nabla e \cdot \mathbf{n}] - \beta_1 \{e\} = 0, \tag{7a}$$
$$[e] = 0. \tag{7b}$$

Impedance transmission conditions of type I are for example the so called ITC-1-0 and ITC-1-1, both derived by asymptotic expansions, see [5]-[6], where the only parameter for the two models is given by

$$\beta_1^{\text{ITC-1-0}} = \gamma^2 d, \qquad \beta_1^{\text{ITC-1-1}} = \gamma^2 d \left(1 + \tfrac{1}{6}\gamma^2 d^2\right). \tag{8}$$

The shielding element [7] can be seen as an ITC similar to (7) with an additional term of the form $\partial_\Gamma^2\{e\}$ arising in (7a).

B. Impedance transmission conditions of type II

Currently, the best known thin sheet conditions are those from [10] (abbreviated by MB in this work), which are based on a similar idea as [9]. They have the form

$$[\nabla e \cdot \mathbf{n}] - \beta_1 \{e\} = 0, \tag{9a}$$
$$[e] - \beta_2 \{\nabla e \cdot \mathbf{n}\} = 0, \tag{9b}$$

where

$$\beta_1^{\text{MB}} = 2\gamma \tanh(\gamma \tfrac{d}{2}), \qquad \beta_2^{\text{MB}} = \tfrac{2}{\gamma} \tanh(\gamma \tfrac{d}{2}). \tag{10}$$

In [6] it has been shown that these conditions even with their more complex structure do not improve the accuracy to the simple ITC-1-0 or the shielding element [7]. An improvement for both, large and small skin-depth to sheet thickness ratios can be observed by choosing [6]

$$\beta_1^{\text{ITC-2-1}} = \frac{2\gamma \sinh\left(\gamma \frac{d}{2}\right)}{\cosh\left(\gamma \frac{d}{2}\right) - \gamma \frac{d}{2} \sinh\left(\gamma \frac{d}{2}\right)}, \tag{11}$$
$$\beta_2^{\text{ITC-2-1}} = -d\left(1 - \tfrac{2}{\gamma d} \tanh(\gamma \tfrac{d}{2})\right),$$

at least for flat sheets. For curved sheets the conditions ITC-2-1 include further terms including the curvature, and do not possess the relatively simple structure (9) anymore.

III. Boundary integral formulations

As the differential equation (3) is extended up to the interface Γ, we can represent the solution in $\mathbb{R}^2 \backslash \Gamma$ as [11]

$$e(\mathbf{x}) = -\int_\Gamma G(\mathbf{x}-\mathbf{y})\,[\nabla e \cdot \mathbf{n}](\mathbf{y})\,\mathrm{d}\Gamma(\mathbf{y}) + \int_\Gamma \mathbf{n} \cdot \nabla_{\mathbf{y}} G(\mathbf{x}-\mathbf{y})\,[e](\mathbf{y})\,\mathrm{d}\Gamma(\mathbf{y}) + N(\mathbf{x}), \tag{12}$$

where we use the Green's kernel $G(\mathbf{x}-\mathbf{y}) = -1/(2\pi)\log(|\mathbf{x}-\mathbf{y}|)$ and the Newton potential

$$N(\mathbf{x}) = \mathrm{i}\omega\mu_0 \int_{\mathbb{R}^2} G(\mathbf{x}-\mathbf{y})\, j_0(\mathbf{y})\,\mathrm{d}\mathbf{y}. \tag{13}$$

A. Boundary integral formulation for the ITCs of type I

The jump of the electric field vanishes and evaluating $e(\mathbf{x})$ in (12) for $\mathbf{x} \to \Gamma$ we obtain for the new unknown $\phi = [\nabla e \cdot \mathbf{n}]$

$$\{e\}(\mathbf{x}) = -\int_\Gamma G(\mathbf{x}-\mathbf{y})\,\phi(\mathbf{y})\,\mathrm{d}\Gamma(\mathbf{y}) + N(\mathbf{x}). \tag{14}$$

Multiplying this equation by β_1 and inserting (7a) gives the integral equation defining $\phi \in L^2(\Gamma)$

$$\phi(\mathbf{x}) + \beta_1 \int_\Gamma G(\mathbf{x}-\mathbf{y})\,\phi(\mathbf{y})\,\mathrm{d}\Gamma(\mathbf{y}) = \beta_1 N(\mathbf{x}). \tag{15}$$

With the single layer operator $V : \phi \mapsto \int_\Gamma G(\mathbf{x}-\mathbf{y})\,\phi(\mathbf{y})\,\mathrm{d}\Gamma(\mathbf{y})$ we can write (15) in variational form

$$\langle \phi, \phi' \rangle + \beta_1 \langle V\phi, \phi' \rangle = \beta_1 \langle N, \phi' \rangle \quad \forall \phi' \in L^2(\Gamma). \tag{16}$$

The integral equation is of second kind, *i. e.*, the associated operator is the sum of identity and a compact perturbation which leads to system matrices for Galerkin boundary element methods (BEM) with condition number bounded independently of the mesh width. See [12] for another boundary integral equation for ITCs of type I.

B. Boundary integral formulation for the ITCs of type II

Taking the mean of the limits $\mathbf{x} \to \Gamma$ from the two sides and inserting (9) we get the mixed integral formulation of second kind for the two unknowns $\phi = [\nabla e \cdot \mathbf{n}]$ and $\psi = [e]$

$$\phi(\mathbf{x}) + \beta_1 \int_\Gamma G(\mathbf{x}-\mathbf{y})\,\phi(\mathbf{y})\,\mathrm{d}\Gamma(\mathbf{y}) - \beta_1 \Big\{ \int_\Gamma \mathbf{n} \cdot \nabla_{\mathbf{y}} G(\mathbf{x}-\mathbf{y})\,\psi(\mathbf{y})\,\mathrm{d}\Gamma(\mathbf{y}) \Big\} = \beta_1 N(\mathbf{x}), \tag{17a}$$

$$\psi(\mathbf{x}) + \beta_2 \Big\{ \mathbf{n} \cdot \nabla_{\mathbf{x}} \int_\Gamma G(\mathbf{x}-\mathbf{y})\,\phi(\mathbf{y})\,\mathrm{d}\Gamma(\mathbf{y}) \Big\} - \beta_2\, \mathbf{n} \cdot \nabla_{\mathbf{x}} \int_\Gamma \mathbf{n} \cdot \nabla_{\mathbf{y}} G(\mathbf{x}-\mathbf{y})\,\psi(\mathbf{y})\,\mathrm{d}\Gamma(\mathbf{y}) = \beta_2 \nabla_{\mathbf{x}} N(\mathbf{x}) \cdot \mathbf{n}. \tag{17b}$$

		ITC-1-0 with $V_h = S_0(\Gamma_h)$		ITC-1-0 with $V_h = S_1(\Gamma_h)$		ITC-1-1 with $V_h = S_0(\Gamma_h)$		ITC-1-1 with $V_h = S_1(\Gamma_h)$	
ndof	h	$\mathrm{SE}_{\mathrm{ITC},h}$	$\lvert\mathrm{SE}_{\mathrm{ITC},h} - \mathrm{SE}_{\mathrm{ITC}}\rvert$	$\mathrm{SE}_{\mathrm{ITC},h}$	$\lvert\mathrm{SE}_{\mathrm{ITC},h} - \mathrm{SE}_{\mathrm{ITC}}\rvert$	$\mathrm{SE}_{\mathrm{ITC},h}$	$\lvert\mathrm{SE}_{\mathrm{ITC},h} - \mathrm{SE}_{\mathrm{ITC}}\rvert$	$\mathrm{SE}_{\mathrm{ITC},h}$	$\lvert\mathrm{SE}_{\mathrm{ITC},h} - \mathrm{SE}_{\mathrm{ITC}}\rvert$
10	37.08 mm	6.7441 dB	0.6552 dB	6.8907 dB	0.5086 dB	6.5385 dB	0.6999 dB	6.7065 dB	0.5319 dB
20	18.64 mm	7.2830 dB	0.1163 dB	7.2822 dB	0.1171 dB	7.1126 dB	0.1258 dB	7.1180 dB	0.1204 dB
40	9.40 mm	7.3735 dB	0.0258 dB	7.3715 dB	0.0278 dB	7.2103 dB	0.0281 dB	7.2098 dB	0.0286 dB
80	4.71 mm	7.3937 dB	0.0056 dB	7.3929 dB	0.0064 dB	7.2320 dB	0.0064 dB	7.2317 dB	0.0067 dB
160	2.36 mm	7.3984 dB	0.0009 dB	7.3984 dB	0.0009 dB	7.2374 dB	0.0010 dB	7.2373 dB	0.0011 dB
320	1.18 mm	7.3994 dB	0.0001 dB	7.3995 dB	0.0002 dB	7.2386 dB	0.0002 dB	7.2386 dB	0.0002 dB
		SE	$\lvert\mathrm{SE} - \mathrm{SE}_{\mathrm{ITC}}\rvert$	SE	$\lvert\mathrm{SE} - \mathrm{SE}_{\mathrm{ITC}}\rvert$	SE	$\lvert\mathrm{SE} - \mathrm{SE}_{\mathrm{ITC}}\rvert$	SE	$\lvert\mathrm{SE} - \mathrm{SE}_{\mathrm{ITC}}\rvert$
		7.2373 dB	0.1620 dB	7.2373 dB	0.1620 dB	7.2373 dB	0.0011 dB	7.2373 dB	0.0011 dB

Table I: Shielding efficiencies $\mathrm{SE}_{\mathrm{ITC},h}$ computed with the integral equations of type I on basis of the impedance transmission conditions ITC-1-0 and ITC-1-1 and their discretisation and modelling error. Reference shielding efficiencies for the original model SE and with ITCs $\mathrm{SE}_{\mathrm{ITC}}$ were computed using high-order FEM. The sheet has an ellipse with semi-axes 60 mm and 38.7 mm as mid-line and a thickness $d = 3$ mm.

With the single layer operator V, the double layer operator $K : \psi \mapsto \left\{ \int_\Gamma \mathbf{n} \cdot \nabla_{\mathbf{y}} G(\mathbf{x} - \mathbf{y})\, \psi(\mathbf{y})\, \mathrm{d}\Gamma(\mathbf{y}) \right\}$, which is the mean of the usual one-sided double layer operators $K^{\pm}$, the adjoint double layer operator $K' : \phi \mapsto \left\{ \mathbf{n} \cdot \nabla_{\mathbf{x}} \int_\Gamma G(\mathbf{x} - \mathbf{y})\, \phi(\mathbf{y})\, \mathrm{d}\Gamma(\mathbf{y}) \right\}$, which is the mean of the usual one-sided adjoint double layer operators $(K')^{\pm}$, and with the hypersingular operator $W : \psi \mapsto -\mathbf{n} \cdot \nabla_{\mathbf{x}} \int_\Gamma \mathbf{n} \cdot \nabla_{\mathbf{y}} G(\mathbf{x} - \mathbf{y})\, \psi(\mathbf{y})\, \mathrm{d}\Gamma(\mathbf{y})$ we can write (17) in variational form: Seek $(\phi, \psi) \in L^2(\Gamma) \times H^{1/2}(\Gamma)$ such that for all $(\phi', \psi') \in L^2(\Gamma) \times H^{1/2}(\Gamma)$

$$\langle \phi, \phi' \rangle + \beta_1 \langle V\phi, \phi' \rangle - \beta_1 \langle K\psi, \phi' \rangle = \beta_1 \langle \gamma_0 NF, \phi' \rangle\,, \quad (18a)$$

$$\beta_2 \langle K'\phi, \psi' \rangle + \langle \psi, \psi' \rangle + \beta_2 \langle W\psi, \psi' \rangle = \beta_2 \langle \gamma_1 NF, \psi' \rangle\,. \quad (18b)$$

This system of integral equations is also of second kind and a Galerkin boundary element discretisation leads to condition numbers, which do not blow up while refining the mesh. Nevertheless, this may be a theoretical result as the integral equations are singularly perturbed, which is due to the small number β_2 in front of W, the highest operator in the system. Hence, the $H^{1/2}(\Gamma)$-norm of ψ may take large values if (i) β_2 takes small values, and (ii) the sheet is not smooth enough [13]. In any case, for the thin sheet conditions [10] and the impedance conditions ITC-2-1 there is a unique solution $(\phi, \psi) \in L^2(\Gamma) \times H^{1/2}(\Gamma)$.

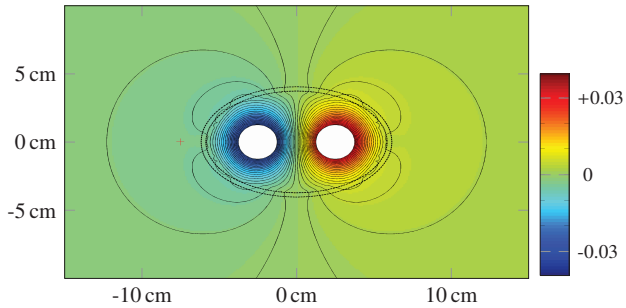

Figure 2: Flux lines and magnitude of magnetic field for an elliptic thin sheet (dashed lines) computed by the integral equation (16) and ITC-1-0. The red cross indicates the point $(-7.5\,\mathrm{cm}, 0\,\mathrm{cm})$ where we study the shielding efficiency.

IV. Asymptotic boundary element methods

We propose Galerkin boundary element methods for the variational formulations (16) and (18). As test and trial functions for the ITCs of type I (15) we may use piecewise constants functions

$$S_0(\Gamma_h) := \left\{ v_h \in L^2(\Gamma) : v_h \in \mathbb{P}_0(K_j),\, j = 1, \ldots, N_h \right\},$$

on a panelisation Γ_h of Γ with N_h straight panels K_j of maximal length h or piecewise linear, continuous functions

$$S_1(\Gamma_h) := \left\{ v_h \in L^2(\Gamma) \cap C(\Gamma) : v_h \in \mathbb{P}_1(K_j),\, j = 1, \ldots, N_h \right\},$$

where the discretisation error in the $L^2(\Gamma)$-norm decays like $O(h)$ using $S_0^{-1}(\Gamma_h)$ and, if the solution has higher smoothness due to smoothness of Γ, like $O(h^2)$ using $S_1^0(\Gamma_h)$. For the ITCs of type II (15) we may use either $S_0^{-1}(\Gamma_h)$ or $S_1^0(\Gamma_h)$ for ϕ and we are obliged to use $S_1^0(\Gamma_h)$ for ψ, where the convergence rates follow accordingly. The straight panels approximate the interface Γ the better the smaller h, and it is well-known that the error induced by the approximation of the geometry is at worst of the same order as the discretisation error [11, Chap. 8].

V. Numerical experiments

We will study the integral equations of type I and II by numerical experiments for a model problem of a thin conducting sheet of thickness $d = 3$ mm, whose mid-line is an ellipse with semi-axes 60 mm and 38.7 mm. The excitation is by two cylindrical current carrying wires with radius 12.5 mm moved to left and right by 25 mm) from the mid-point of the ellipse and with $j_0 = \pm 1$ (arbitrary units), see the schematic sketch in Fig. 1. We choose a frequency of 50 Hz ($\omega = 314\,\mathrm{rad/s}$), a copper sheet with $\sigma = 5.91 \cdot 10^7\,\mathrm{A(Vm)^{-1}}$ and $\mu = \mu_0$, for which the skin depth is with 9.26 mm about three times larger than the thickness.

Reference solutions for the original model resolving the thin sheet and the model with ITCs were computed using a high order FEM discretisation, where the edges of the quadrilaterals cells follow exactly the curvature of the thin sheet. For this we used the numerical C++ library Concepts [14], see also `www.concepts.math.ethz.ch`. As we stated the problem in the unbounded space $\mathbb{R}^2$ we use exact Dirichlet-to-Neumann maps on the circular boundary of a

		MB with $V_h = S_0(\Gamma_h)$		MB with $V_h = S_1(\Gamma_h)$		ITC-2-1 with $V_h = S_0(\Gamma_h)$		ITC-2-1 with $V_h = S_1(\Gamma_h)$	
ndof	h	$\mathrm{SE}_{\mathrm{ITC},h}$	$\lvert\mathrm{SE}_{\mathrm{ITC},h} - \mathrm{SE}_{\mathrm{ITC}}\rvert$	$\mathrm{SE}_{\mathrm{ITC},h}$	$\lvert\mathrm{SE}_{\mathrm{ITC},h} - \mathrm{SE}_{\mathrm{ITC}}\rvert$	$\mathrm{SE}_{\mathrm{ITC},h}$	$\lvert\mathrm{SE}_{\mathrm{ITC},h} - \mathrm{SE}_{\mathrm{ITC}}\rvert$	$\mathrm{SE}_{\mathrm{ITC},h}$	$\lvert\mathrm{SE}_{\mathrm{ITC},h} - \mathrm{SE}_{\mathrm{ITC}}\rvert$
10	37.08 mm	6.9389 dB	0.6531 dB	7.0929 dB	0.4990 dB	6.5357 dB	0.6978 dB	6.7039 dB	0.5296 dB
20	18.64 mm	7.4783 dB	0.1136 dB	7.4800 dB	0.1119 dB	7.1082 dB	0.1253 dB	7.1136 dB	0.1199 dB
40	9.40 mm	7.5669 dB	0.0250 dB	7.5654 dB	0.0266 dB	7.2054 dB	0.0281 dB	7.2050 dB	0.0285 dB
80	4.71 mm	7.5864 dB	0.0055 dB	7.5858 dB	0.0061 dB	7.2272 dB	0.0063 dB	7.2269 dB	0.0066 dB
160	2.36 mm	7.5910 dB	0.0009 dB	7.5907 dB	0.0012 dB	7.2324 dB	0.0011 dB	7.2323 dB	0.0012 dB
320	1.18 mm	7.5922 dB	0.0003 dB	7.5922 dB	0.0003 dB	7.2338 dB	0.0003 dB	7.2333 dB	0.0002 dB
		SE	$\lvert\mathrm{SE} - \mathrm{SE}_{\mathrm{ITC}}\rvert$	SE	$\lvert\mathrm{SE} - \mathrm{SE}_{\mathrm{ITC}}\rvert$	SE	$\lvert\mathrm{SE} - \mathrm{SE}_{\mathrm{ITC}}\rvert$	SE	$\lvert\mathrm{SE} - \mathrm{SE}_{\mathrm{ITC}}\rvert$
		7.2373 dB	0.3547 dB	7.2373 dB	0.3547 dB	7.2373 dB	0.0038 dB	7.2373 dB	0.0038 dB

Table II: Shielding efficiencies $\mathrm{SE}_{\mathrm{ITC},h}$ computed with the integral equations of type I on basis of the thin sheet conditions and ITC-2-1 and their discretisation and modelling error (same thin sheet as in Table I). Reference shielding efficiencies for the original model SE and with ITCs $\mathrm{SE}_{\mathrm{ITC}}$ were computed using high-order FEM.

bounded computational domain. Note, that a modelling error is introduced by using the ITCs instead of modelling the thin conducting sheet, by which both, the reference solution and the BEM solution are affected. When studying the discretisation error we will compare the solution of the proposed BEM for the different ITCs with their respective reference solution.

First, we study the influence of the discretisation error for the integral equations of type I to the shielding efficiency evaluated at the point $(-7.5\,\mathrm{mm}, 0\,\mathrm{mm})$, see Table I. For both piecewise constant and piecewise linear continuous functions the numerical shielding efficiencies $\mathrm{SE}_{\mathrm{ITC},h}$ converge for decreasing mesh widths h to 7.3993 dB for ITC-1-0 and 7.2384 dB for ITC-1-1. The shielding efficiency has a logarithmic dependence on the solution and is therefore not a usual quantity for theoretical estimates of the discretisation error. We observe with both discrete spaces $S_0(\Gamma_h)$ and $S_1(\Gamma_h)$ more than quadratic convergence, where the error with $S_1(\Gamma_h)$ is lower than with $S_0(\Gamma_h)$ only for 10 panels and for finer discretisations the errors do not differ much. The exact shield efficiency is, however, 7.2373 dB, and with a mesh consisting of 20 panels the discretisation error for the integral equation with ITC-1-0 is already below the modelling error of 0.1620 dB. For ITC-1-1 the modelling error is only 0.0011 dB and refinement up to a mesh width $h = 2.36\,\mathrm{mm}$ is meaningful.

Second, we study the influence of the discretisation error for the integral equations of type II to the shielding efficiency, which we again evaluate at $(-1.5, 0)$ see Table II. We use the thin sheet conditions (MB) and ITC-2-1, knowing that the latter has a more complex structure due to curvature terms, which we neglect here. The numerical shielding efficiencies $\mathrm{SE}_{\mathrm{ITC},h}$ converge with $h \to 0$ to 7.5919 dB for the thin sheet conditions and to 7.2335 dB for ITC-2-1, independent if $V_h = S_0(\Gamma_h)$ or $V_h = S_1(\Gamma_h)$. The discretisation errors for the integral equations of type II are very close to the respective values of type I. The limit values of the shielding efficiency for $h \to 0$ differ from those of the model resolving the thin sheet by 0.3547 dB for the thin sheet conditions, and by 0.0038 dB for ITC-2-1. In this example a mesh refinement does not lead to a reduction of the total error if h is already 18.64 mm for the thin sheet conditions or 2.36 mm for ITC-2-1.

VI. Conclusion

We proposed and analysed boundary integral equations of two types for impedance transmission conditions, which replace thin conducting sheets in order to avoid the numerical difficulties due to the small distance of the two sheet surfaces. The integral equations turn out to be of second kind. However, the integral equations of type II are singularly perturbed. Numerically we studied the influence of the discretisation error on the shielding efficiency, for which we obtain convergence in the mesh width. As there is still a modelling error the method does not converge to the exact physical shielding efficiency. The total error can only be further reduced if an improved impedance transmission condition is used.

References

[1] K. Schmidt, O. Sterz, and R. Hiptmair, "Estimating the eddy-current modelling error," *IEEE Trans. Magn.*, vol. 44, no. 6, pp. 686–689, 2008.

[2] S. Celozzi, G. Lovat, and R. Araneo, *Electromagnetic Shielding*. New York, USA: John Wiley & Sons, Inc., 2001.

[3] T. Levi-Civita, "La teoria elettrodinamica di Hertz di fronte ai fenomeni di induzione," *Rend. Lincei (5)*, vol. 11, no. 2, pp. 75–81, 1902, (in Italian).

[4] K. Schmidt and S. Tordeux, "Asymptotic modelling of conductive thin sheets," *Z. Angew. Math. Phys.*, vol. 61, no. 4, pp. 603–626, 2010.

[5] ——, "High order transmission conditions for thin conductive sheets in magneto-quasistatics," *ESAIM: M2AN*, vol. 45, no. 6, pp. 1115–1140, 2011.

[6] K. Schmidt and A. Chernov, "A unified analysis of transmission conditions for thin conducting sheets in the time-harmonic eddy current model," accepted for publication in SIAM J. Appl. Math., 2013.

[7] T. Nakata, N. Takahashi, K. Fujiwara, and Y. Shiraki, "3D magnetic field analysis using special elements," *IEEE Trans. Magn.*, vol. 26, no. 5, pp. 2379–2381, 1990.

[8] O. Tozoni and I. Mayergoyz, *Calculation of three-dimensional electromagnetic fields*. Kiev: Technika, 1974, (in Russian).

[9] L. Krähenbühl and D. Muller, "Thin layers in electrial engineering. Example of shell models in analysing eddy-currents by boundary and finite element methods," *IEEE Trans. Magn.*, vol. 29, no. 2, pp. 1450–1455, 1993.

[10] I. Mayergoyz and G. Bedrosian, "On calculation of 3-D eddy currents in conducting and magnetic shells," *IEEE Trans. Magn.*, vol. 31, no. 3, pp. 1319–1324, 1995.

[11] S. Sauter and C. Schwab, *Boundary element methods*. Berlin & Heidelberg, Germany: Springer-Verlag, 2011.

[12] H. Igarashi, A. Kost, and T. Honma, "Impedance boundary condition for vector potentials on thin layers and its application to integral equations," *Eur. Phys. J. AP*, vol. 1, pp. 103–109, 1998.

[13] K. Schmidt and R. Hiptmair, "Asymptotic boundary element methods for thin conducting sheets," Institut für Mathematik, TU Berlin, Preprint 15-2013, 2013.

[14] P. Frauenfelder and C. Lage, "Concepts – An Object-Oriented Software Package for Partial Differential Equations," *Math. Model. Numer. Anal.*, vol. 36, no. 5, pp. 937–951, 2002.